

# Enhanced B2 Ordering of FeRh Thin Films Using B2 NiAl Underlayers

Dhishan Kande<sup>1,2</sup>, Simone Pisana<sup>3</sup>, Dieter Weller<sup>3</sup>, David E. Laughlin<sup>1,2</sup>, and Jian-Gang Zhu<sup>3,4</sup>, *Fellow, IEEE*

<sup>1</sup>Department of Materials Science and Engineering, Carnegie Mellon University, Pittsburgh, PA 15213 USA

<sup>2</sup>Data Storage Systems Center, Carnegie Mellon University, Pittsburgh, PA 15213 USA

<sup>3</sup>San Jose Research Center, Hitachi Global Storage Technologies, San Jose, CA 95135 USA

<sup>4</sup>Department of Electrical and Computer Engineering, Carnegie Mellon University, Pittsburgh, PA 15213 USA

**B2-ordered FeRh thin films undergo a first-order magnetic transition from an antiferromagnetic (AFM) state at low temperature to a ferromagnetic (FM) state above 350 K and reverse back on cooling with a finite hysteresis. This property makes them very attractive for use in temperature-controlled exchange coupling layers for heat-assisted magnetic recording. In order to be used as an exchange coupling layer, the goal is to fabricate ultra-thin films of FeRh that show reversible AFM-FM switching. For thinner films grown on MgO substrates, there exists an FM signal below the AFM-FM transition temperature. It is demonstrated that there is a direct correlation between the low-temperature FM fraction and the extent of atomic ordering. Based on this observation, the enhanced atomic order in FeRh grown on NiAl underlayers is shown to result in bulk-like AFM-FM switching, especially for the thinner films.**

*Index Terms*—Iron alloys, magnetic layered films, thermomagnetic recording, thin films.

## I. INTRODUCTION

FeRh of the B2 structure in the bulk form shows a unique thermomagnetic transition [1] in a narrow composition range. The alloy is antiferromagnetic (AFM) at room temperature and undergoes an abrupt transition to a ferromagnetic (FM) state above 350 K, and this transition reverses on cooling with a finite hysteresis. This property has created interest in thin films of this material to be used for temperature-controlled exchange coupling layers in heat-assisted magnetic recording (HAMR) [2], [3] and magnetic random access memory applications [4], [5]. The primary objective of our research is to be able to grow ultra-thin FeRh films for controlled exchange coupling between two magnetic layers. For this kind of application, it is important to have a very thin FeRh film that is AFM at room temperature leading to negligible coupling of the magnetic layers to begin with. Studies on growth of thicker FeRh films [6]–[9] have shown that only the films postannealed above 770 K have low FM phase fractions below the respective AFM-FM transition temperature. It has also been observed that thinner films [10] with Rh-richer compositions (>55 at.% Rh) have residual FM signals below the AFM-FM transition temperature. These films had low atomic (or chemical) ordering possibly due to phase separation. In this paper, we demonstrate that growing FeRh thin films on NiAl underlayers leads to an increase in atomic ordering of the FeRh. Minimal FM fraction was found in these films at room temperature and the AFM-FM switching was bulk-like. We also show a widely applicable correlation between the atomic-order parameter and the FM fraction below the AFM-FM transition temperature. This dependence could help in understanding why the AFM-FM switching in FeRh thin films is better in certain cases and not in others.

## II. EXPERIMENT

FeRh thin films were grown by two sputtering techniques. This was done to demonstrate that the effect of chemical ordering on the AFM-FM transition is general to any method of fabrication. The first series of samples were grown by dc magnetron confocal cosputtering from elemental Fe and Rh targets on to MgO (0 0 1) single crystal substrates at 300 K and 5 mT argon pressure. Then, the films were postannealed at 800 K for 2 h inside the sputtering system. The other set of samples were deposited by radio frequency (RF) alternate layer sputtering of Fe and Rh on to a heated MgO(0 0 1) substrate at 800 K. The argon pressure for sputtering was 20 mT for this method. The higher pressure was used to create a rough Fe/Rh interface that aids the diffusion kinetics and improves compositional homogenization. To study the effect of the NiAl underlayer, first a thickness series was made of [Fe/Rh] directly on MgO(0 0 1) substrates and identical conditions were used to deposit the same on an NiAl underlayer at 800 K. The NiAl underlayer was deposited on to the MgO(0 0 1) substrate at 800 K and 10 mT argon pressure.

The thickness of the films measured by X-ray reflectivity, and the out of plane X-ray diffraction measurements were both performed in the Philips X'pert diffractometer. The order parameter in this paper is defined as the square root of integrated intensity ratios of the superlattice (0 0 1) B2 peak to the fundamental (0 0 2) B2 peak, corrected for thickness-dependent absorption only. While calculating the latter, the absorption coefficient of the alloy was taken to be the weighted mean (by composition) of the elemental absorption coefficients of Fe and Rh for a Cu K $\alpha$  radiation. The area under the peaks was calculated using the peak fitting program in Origin 6.1. Linear background subtraction was used before measuring the areas. It is to be noted that it is not abnormal to get measured integrated intensity ratio in thin films to be greater than one [11]. Average composition of the thin films was measured by the energy dispersive spectroscopy in the Philips XL-30 scanning electron microscope. The magnetic measurements were performed in a physical property measurement system (PPMS) as well as a superconducting quantum interference device (SQUID). These measurements were performed by applying an in-plane saturating field and measuring

Manuscript received February 21, 2011; revised April 30, 2011; accepted May 21, 2011. Date of current version September 23, 2011. Corresponding author: D. Kande (e-mail: dkande@andrew.cmu.edu).

Color versions of one or more of the figures in this paper are available online at <http://ieeexplore.ieee.org>.

Digital Object Identifier 10.1109/TMAG.2011.2157963

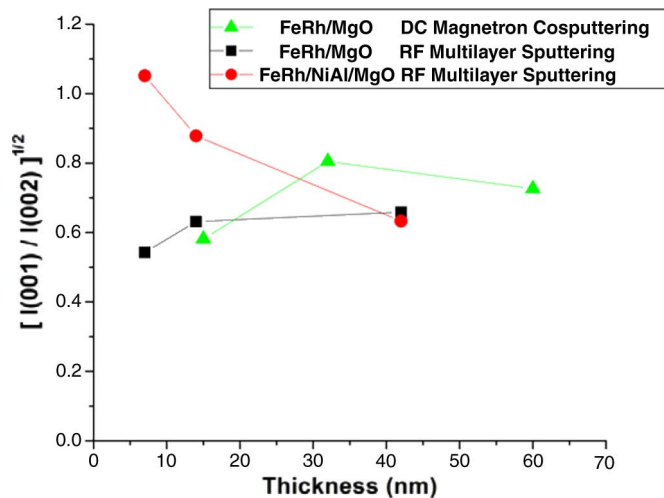


Fig. 1. Atomic order versus thickness. (Average composition of FeRh for all films: 47 at.% Fe–53 at.%Rh.)

magnetic moment as a function temperature. The FM fraction at 200 K was chosen for comparing different samples. This fraction was obtained by normalizing the moment at 200 K to the maximum moment in the moment versus temperature measurement for every sample.

### III. RESULTS AND DISCUSSION

Fig. 1 shows the dependence of atomic ordering on the thickness of the FeRh films. All these films had an average composition of 53 at.% Rh. For the FeRh films grown on MgO(0 0 1) substrates, there was a decrease in the atomic order at lower thicknesses. However, for the films grown on top of the B2 NiAl underlayer, the ordering increased with decreasing thickness. This could be due to stress assisted ordering. The strain energy from the lattice mismatch can alter the energetics of the nucleation of the B2-ordered phase and lead to higher atomic ordering [12], [13]. Also, since the NiAl lattice has the same B2 structure as the FeRh only with a smaller lattice constant, thinner the FeRh film greater the tendency of the Fe and Rh atoms to form an ordered B2 structure on the B2 NiAl template. The 42 nm FeRh film grown on MgO as well as NiAl had similar atomic-order parameters. This is because the stress is relaxed in the thicker film in both cases. However, the thinner films had very different atomic-order parameters and one reason could be that the stress was not fully relaxed across the thickness of the film. There could also be a change in atomic ordering due to diffusion at the film–substrate interface. In this paper, we focus on the “effect” and not the “origin” of atomic disorder. Inter-diffusion studies at the FeRh/NiAl interface as well as the FeRh/MgO interface are being currently explored by X-ray photoelectron spectroscopy (XPS) as a separate systematic study. In general, the dependence of atomic order on thickness is an outcome of the interplay between the effects of inter-diffusion, underlayer template effect, and film stress. The contributions of these factors could be different based on the method of fabrication and processing.

Fig. 2 shows a comparison of the magnetic switching properties of the 14 nm FeRh film grown on NiAl versus the FeRh film

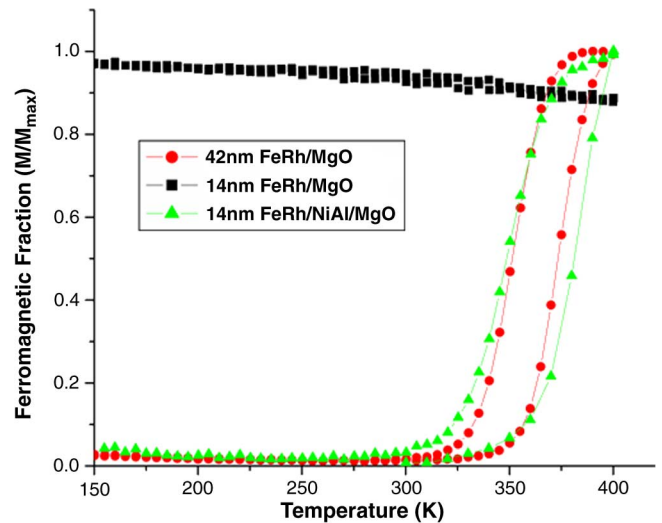


Fig. 2. Effect of NiAl underlayer on AFM-FM switching in the 14 nm FeRh film. (Average composition of FeRh for all three samples: 47 at.% Fe–53 at.%Rh.)

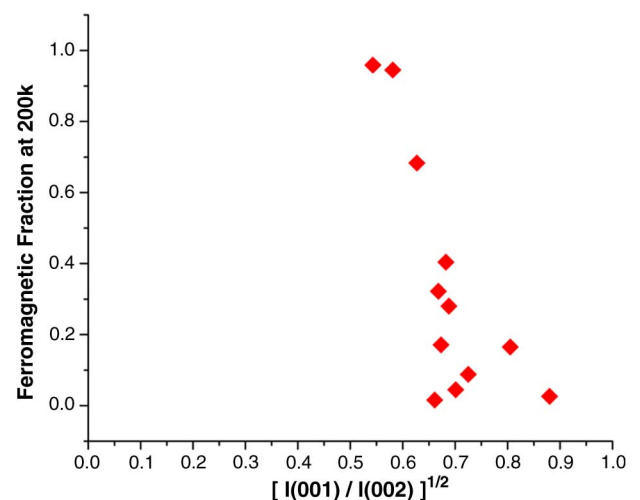


Fig. 3. Correlation between atomic order and residual FM fraction.

grown directly on MgO(0 0 1) substrate. The data from the 42 nm FeRh/MgO(0 0 1) are shown as a reference. The final goal of the research is to eliminate any low-temperature FM signal, and hence, normalized moment (referred to as FM fraction in this paper) is used as a measure of this undesired signal.

It is evident that there is a very small low temperature FM signal in the 14 nm film on NiAl. On the other hand, the 14 nm film on MgO is almost fully FM to begin with. This indicates that there is a correlation between the FM signal at low temperatures and the atomic-order parameter. In order to further confirm this, magnetic data from various samples made at Carnegie Mellon University, Pittsburgh, PA, as well as the Hitachi Global Storage Technologies, San Jose, CA, were plotted as shown in Fig. 3. It is a plot of the FM fraction (at 200 K) as a function of chemical-order parameter for samples with different thicknesses (14–42 nm), different alloy compositions (53–60 at.% Rh), and made by either of the two fabrication methods (RF or dc sputtering). The broad applicability of this dependence shows that

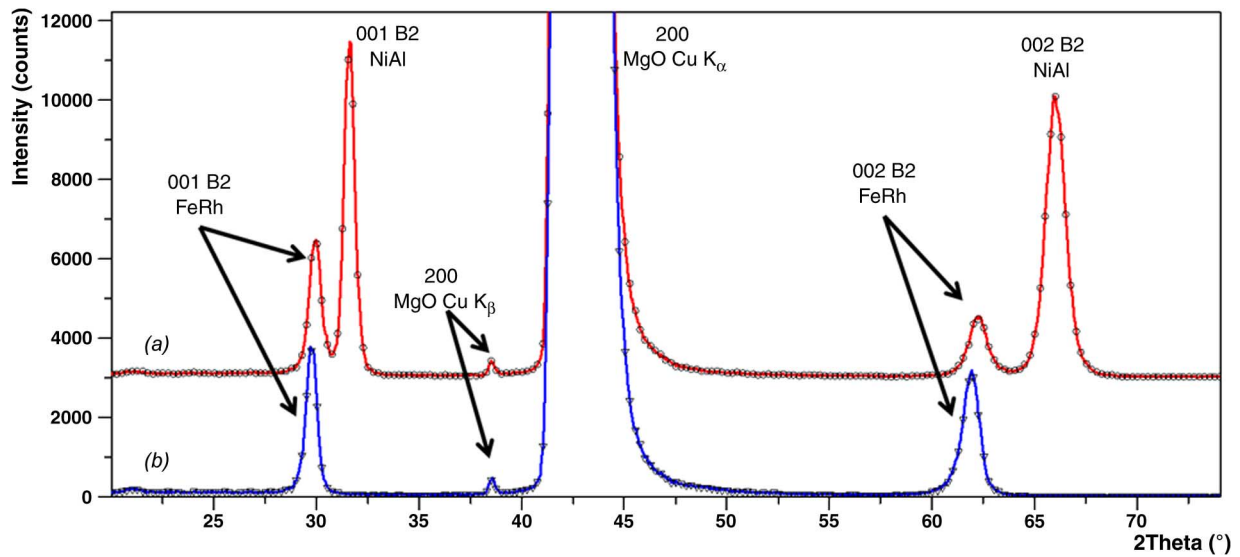


Fig. 4. Out of plane XRD scans of (a) 14 nm FeRh/NiAl/MgO,  $c$  (B2 FeRh) = 2.981 Å and (b) 14 nm FeRh/MgO,  $c$  (B2 FeRh) = 2.998 Å.

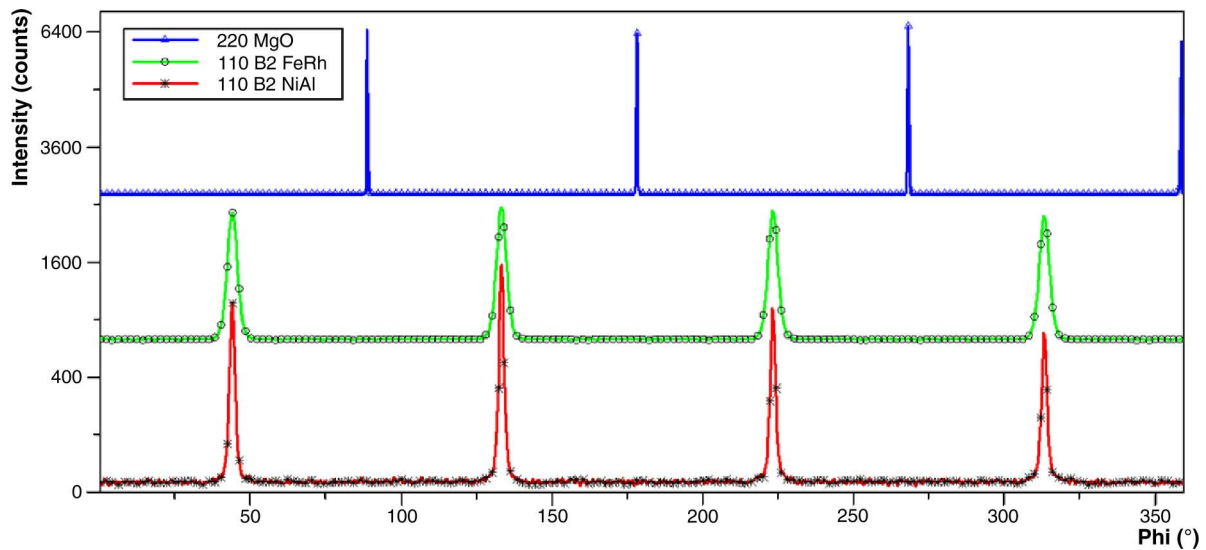


Fig. 5.  $\varphi$  scans showing the orientation relationships between the FeRh, NiAl, and MgO lattices.

the atomic disorder leads to residual FM signal. From the equilibrium phase diagram of Fe-Rh [14], it is seen that the AFM B2 phase ( $\alpha''$ ) exists beyond 50 at.% Rh. Below that Rh content, even complete chemical ordering would only yield an FM B2 phase ( $\alpha'$ ) [15]. Hence, only the films with compositions beyond 52 at.% Rh were considered for the plot in Fig. 3. Also, by picking compositions in the two phase field of  $\alpha''$  (AFM) and  $\gamma$  (>52 at.% Rh), any change in alloy composition does not change the equilibrium  $\alpha''$  composition. Thus, the composition dependence of atomic order is absent in our study.

The scatter in the data could be accounted by the fact that a part of the measurements were performed in the SQUID and the rest in the PPMS, and the saturation fields applied were 0.8 and 2 T, respectively. There is a weak dependence of the FM fraction on the saturating field applied [16]–[18].

Fig. 4 shows the out of plane X-ray diffraction (XRD) data for the 14 nm FeRh film with and without the NiAl underlayer. B2 NiAl sputtered on to heated MgO(0 0 1) substrates

grows with the (0 0 1) texture and a lattice constant of 2.83 Å. The B2 FeRh has a bulk lattice constant of 2.99 Å but when grown on the NiAl had a lower lattice constant of 2.98 Å indicating that it was indeed strained by the underlayer. In the case of growth on MgO, the mismatch between the bulk B2 FeRh (2.99 Å) lattice and the rotated MgO lattice ( $4.211/\sqrt{2} = 2.98$  Å) is much smaller. Lattice constants were measured from the (0 0 2) peak of the B2 phase to reduce error due to overlap with the (0 0 2) NiAl peak. It can also be inferred from this figure that the  $I(0 0 1)/I(0 0 2)$  is larger in the case with NiAl underlayer.

By using  $\varphi$  scans at  $\psi = 45^\circ$ , the relative orientations of the FeRh, NiAl, and MgO lattices are shown in Fig. 5. The NiAl grows such that the lattice is rotated by  $45^\circ$  in the plane relative to the MgO substrate lattice. The FeRh lattice grows exactly matched with the NiAl. The fourfold symmetry for the 110 B2 FeRh and 110 B2 NiAl peaks prove that both of them are single crystalline.

## IV. CONCLUSION

In conclusion, the AFM-FM behavior of FeRh films is directly affected by the extent of atomic order and by using suitable underlayers like NiAl, the atomic order could be enhanced to get bulk-like switching in much thinner FeRh films. However, the 7 nm FeRh film grown on NiAl was not AFM in spite of the higher atomic-order parameter. This indicates that there are other factors like stress uniformity across the film thickness, surface structure, and interdiffusion that could have a critical role to play for the AFM-FM switching in ultra-thin films [19], [20]. This is a topic of our future study.

## ACKNOWLEDGMENT

This work was supported in part by NSF/MRSEC at Johns Hopkins University, the Data Storage Systems Center, Carnegie Mellon University, Pittsburgh, PA, and its industrial sponsors. D. Kande thanks Hitachi Global Storage Technologies, San Jose, CA, for allowing a part of this work to be done during a summer research internship. D. Kande, D. E. Laughlin, and J.-G. Zhu thank Williams Advanced Materials for materials support.

## REFERENCES

- [1] J. S. Kouvel and C. C. Hartelius, "Anomalous magnetic moments and transitions in the ordered alloy FeRh," *J. Appl. Phys.*, vol. 33, pp. 1343–1344, 1962.
- [2] J. Thiele, S. Maat, and E. E. Fullerton, "FeRh/FePt exchange spring films for thermally assisted magnetic recording media," *Appl. Phys. Lett.*, vol. 82, pp. 2859–2861, 2003.
- [3] J.-G. Zhu, "Binary anisotropy media," in *Proc. Annu. Int. Conf. Magn. Mater.*, Tampa, FL, November 5–8, 2007.
- [4] E. Fullerton, S. Maat, and J. U. Thiele, "Heat assisted switching in an MRAM cell utilizing the antiferromagnetic to ferromagnetic transition in FeRh," San Jose, CA U.S. Patent 20 050 281 081.
- [5] J.-G. Zhu, Y. Luo, and X. Li, "Crossbar diode-switched magnetoresistive random access memory system," Pittsburgh, PA U.S. Patent 7 826 258.
- [6] J. Cao, N. T. Nam, S. Inoue, H. Y. Y. Ko, N. N. Phuoc, and T. Suzuki, "Magnetization behaviors for FeRh single crystal thin films," *J. Appl. Phys.*, vol. 103, pp. 07F501-1–07F501-3, 2008.
- [7] S. Hashi, S. Yanase, Y. Okazaki, and M. Inoue, "A large thermal elasticity of the ordered FeRh alloy film with sharp magnetic transition," *IEEE Trans. Magn.*, vol. 40, no. 4, pp. 2784–2786, Jul. 2004.
- [8] Y. Ohtani and I. Hatakeyama, "Antiferro-ferromagnetic transition and microstructural properties in a sputter deposited FeRh thin film system," *J. Appl. Phys.*, vol. 74, pp. 3328–3332, 1993.
- [9] J. M. Lommel, "Magnetic and electrical properties of FeRh thin films," *J. Appl. Phys.*, vol. 37, pp. 1483–1484, 1966.
- [10] D. Kande, D. E. Laughlin, and J.-G. Zhu, "Origin of room temperature ferromagnetic moment in Rh-rich [Rh/Fe] multilayer thin films," *J. Appl. Phys.*, vol. 107, pp. 09E318-1–09E318-3, 2010.
- [11] E. Yang, D. E. Laughlin, and J.-G. Zhu, Correction of order parameter calculation for FePt perpendicular thin films to be published.
- [12] S. N. Hsiao, "Effect of initial stress/strain state of the order-disorder transformation of FePt thin films," *Appl. Phys. Lett.*, vol. 94, pp. 232505-1–232505-3, 2009.
- [13] D. A. Porter and K. E. Easterling, *Phase Transformations in Metals and Alloys*, 2nd ed. Boca Raton, FL/London, U.K.: CRC Press/Taylor & Francis, 1992, pp. 287–314.
- [14] T. B. Massalski, *Binary Alloy Phase Diagrams*. Materials Park, OH: ASM Int., 1990, vol. 2, pp. 1760–1760.
- [15] J. van Driel, R. Coehoorn, G. J. Strijkers, E. Brück, and F. R. de Boer, "Compositional dependence of the giant magnetoresistance in  $\text{Fe}_x\text{Rh}_{1-x}$  thin films," *J. Appl. Phys.*, vol. 85, pp. 1026–1036, 1999.
- [16] S. Maat, J. U. Thiele, and E. E. Fullerton, "Temperature and field hysteresis of the antiferromagnetic-to-ferromagnetic phase transition in epitaxial FeRh films," *Phys. Rev. B*, vol. 72, pp. 214432-1–214432-10, 2005.
- [17] M. R. Ibarra and P. A. Algarabel, "Giant volume magnetostriction in the FeRh alloy," *Phys. Rev. B*, vol. 50, pp. 4196–4199, 1994.
- [18] Y. Ohtani and I. Hatakeyama, "Features of broad magnetic transition in FeRh thin film," *J. Magn. Magn. Mater.*, vol. 131, pp. 339–344, 1994.
- [19] R. Fan, C. J. Kinane, T. R. Charlton, R. Dorner, M. Ali, M. A. de Vries, R. M. D. Brydson, and C. H. Marrows, "Ferromagnetism at the interfaces of antiferromagnetic FeRh epilayers," *Phys. Rev. B*, vol. 82, pp. 184418-1–184418-5, 2010.
- [20] D. Kande, A. T. Wise, D. E. Laughlin, and J.-G. Zhu, "Detailed investigation of the first order magnetic phase transition in iron rhodium (FeRh) sputtered thin films," to be published.